1992-12

Study of grain refinement in Al alloy 2519 using backscatter orientation-contrast mode in the scanning electron microscope

Dunlap, Jeffrey Robert

Monterey, California. Naval Postgraduate School

UNCLASSIFIED
SECURITY CLASSIFICATION OF THIS PAGE

REPORT DOCUMENTATION PAGE

1a. REPORT SECURITY CLASSIFICATION UNCLASSIFIED	1b RESTRICTIVE MARKINGS
2a. SECURITY CLASSIFICATION AUTHORITY	3. DISTRIBUTION/AVAILABILITY OF REPORT Approved for public release; distribution is unlimited
2b. DECLASSIFICATION/DOWNGRADING SCHEDULE	
4. PERFORMING ORGANIZATION REPORT NUMBER(S)	5. MONITORING ORGANIZATION REPORT NUMBER(S)
6a. NAME OF PERFORMING ORGANIZATION Naval Postgraduate School 6b. OFFICE SYMBOL (*If applicable*) ME	7a. NAME OF MONITORING ORGANIZATION Naval Postgraduate School
6c. ADDRESS (*City, State, and ZIP Code*) Monterey, CA 93943-5000	7b. ADDRESS (*City, State, and ZIP Code*) Monterey, CA 93943-5000
8a. NAME OF FUNDING/SPONSORING ORGANIZATION 8b. OFFICE SYMBOL (*If applicable*)	9. PROCUREMENT INSTRUMENT IDENTIFICATION NUMBER
8c. ADDRESS (*City, State, and ZIP Code*)	10. SOURCE OF FUNDING NUMBERS Program Element No. / Project No. / Task No. / Work Unit Accession Number

11. TITLE (*Include Security Classification*)
Study of grain refinement in Al alloy 2519 using backscatter orientation-contrast mode in the scanning electron microscope (unclassified)

12. PERSONAL AUTHOR(S) Jeffrey Robert Dunlap

13a. TYPE OF REPORT	13b. TIME COVERED	14. DATE OF REPORT (*year, month, day*)	15. PAGE COUNT
Master's Thesis	From 06/92 To 12/92	December 1992	58

16. SUPPLEMENTARY NOTATION
The views expressed in this thesis are those of the author and do not reflect the official policy or position of the Department of Defense or the U.S. Government.

17. COSATI CODES			18. SUBJECT TERMS (*continue on reverse if necessary and identify by block number*)
FIELD	GROUP	SUBGROUP	Aluminum-Copper alloys, Grain refinement, particle stimulated nucleation (PSN)

19. ABSTRACT (*continue on reverse if necessary and identify by block number*)

The effects of variations in thermomechanical processing (TMP) parameters on grain refinement in 2519 Al-Cu alloy were studied. Refined grains enhance tensile ductility and are a prerequisite for superplastic response. The TMP variables were adjusted based on particle stimulated nucleation (PSN) theory. Process modifications included increased initial overaging time and decreased subsequent warm rolling temperatures. Backscatter orientation-contrast (BSOC) techniques for the scanning electron microscope (SEM) were developed to achieve grain-orientation contrast. An accelerating voltage of 5KV resulted in increased intensities for atomic number and orientation contrast. Both grains and θ-phase (Al_2Cu) precipitates were revealed on the same micrograph at higher resolutions than attainable in the optical microscope. Quantitative data from micrographs were obtained using image analysis methods. A method based on statistical considerations was developed to determine an approximate critical θ-phase particle diameter (d_{cr}) for PSN. The θ-phase particle distribution was shown to be an important factor for grain refinement via PSN.

20. DISTRIBUTION/AVAILABILITY OF ABSTRACT	21. ABSTRACT SECURITY CLASSIFICATION	
☒ UNCLASSIFIED/UNLIMITED ☐ SAME AS REPORT ☐ DTIC USERS	UNCLASSIFIED	
22a. NAME OF RESPONSIBLE INDIVIDUAL Terry R. McNelley	22b. TELEPHONE (*Include Area code*) (408) 646-2589	22c. OFFICE SYMBOL ME/Mc

DD FORM 1473, 84 MAR — 83 APR edition may be used until exhausted; All other editions are obsolete

SECURITY CLASSIFICATION OF THIS PAGE
UNCLASSIFIED

STUDY OF GRAIN REFINEMENT IN Al ALLOY 2519 USING BACKSCATTER ORIENTATION-CONTRAST MODE IN THE SCANNING ELECTRON MICROSCOPE

by
Jeffrey Robert Dunlap
Lieutenant, United States Navy
B.S.M.E, Virginia Polytechnic Institute, 1986

Submitted in partial fulfillment
of the requirements for the degree of

MASTER OF SCIENCE IN MECHANICAL ENGINEERING

from the

NAVAL POSTGRADUATE SCHOOL
December 1992

ABSTRACT

The effects of variations in thermomechanical processing (TMP) parameters on grain refinement in 2519 Al-Cu alloy were studied. Refined grains enhance tensile ductility and are a prerequisite for superplastic response. The TMP variables were adjusted based on particle stimulated nucleation (PSN) theory. Process modifications included increased initial overaging time and decreased subsequent warm rolling temperatures. Backscatter orientation-contrast (BSOC) techniques for the scanning electron microscope (SEM) were developed to achieve grain-orientation contrast. An accelerating voltage of 5KV resulted in increased intensities for atomic number and orientation contrast. Both grains and θ-phase (Al_2Cu) precipitates were revealed on the same micrograph at higher resolutions than attainable in the optical microscope. Quantitative data from micrographs were obtained using image analysis methods. A method based on statistical considerations was developed to determine an approximate critical θ-phase particle diameter (d_{crit}) for PSN. The θ-phase particle distribution was shown to be an important factor for grain refinement via PSN.

TABLE OF CONTENTS

I. INTRODUCTION

Tensile test samples of structural alloys exhibit localized area reduction, or necking, prior to failure of the material. The susceptibility of a material to localized necking during elevated temperature straining is related in part to strain rate sensitivity coefficient, m:

$$m = \frac{\partial \ln \sigma}{\partial \ln \dot{\epsilon}} \tag{1.1}$$

where $\dot{\epsilon}$ is the strain rate and σ is the flow stress. If a material exhibits a low m value, the deformation tends to concentrate in the necked region due to a lack of strain-rate hardening. For larger m values, the material will exhibit strain-rate hardening and this impedes further reductions at the neck. As the material continues to be strained, localized necking is prevented thereby accounting for large elongations without failure. Superplasticity of a material, from an applied mechanics perspective, is an extremely high tensile elongation (>200 pct.) within a defined temperature-strain rate range.

The value of m is influenced by strain rate, temperature and the alloy microstructure. For superplastic deformation, these factors are related by an equation of the form

$$\dot{\epsilon} \propto \frac{D_{eff}}{\delta^2}\left(\frac{\sigma}{E}\right)^{\frac{1}{m}} \qquad (1.2)$$

where D_{eff} is the effective diffusion coefficient, δ is the grain size and E is the modulus of elasticity. A decreased grain size is associated with an increased strain rate and often with a larger m coefficient. This relationship indicates the importance of fine grain size for superplasticity. Superplastic alloys usually exhibit $m \geq 0.3$ in tensile deformation at temperatures typically in the range of 0.5 to 0.7 T_m [Ref. 1], where T_m is the melting temperature. As m increases, the superplastic response improves. Ideal superplastic response occurs when m = 1, i.e., the material behaves in a Newtonian-Viscous manner, whereby diffusional flow dominates and no localized necking occurs [Ref. 2].

Diffusion controls superplastic response. The combination of grain boundary diffusion, D_{gb}, and lattice self-diffusion, D_L, are believed to contribute to the total diffusion according to:

$$D_{eff}=D_L f_L+D_{gb} f_{gb} \qquad (1.3)$$

where f_L and f_{gb} are the fractions of atoms associated with lattice and grain boundary diffusion, respectively. If $f_L= 1$ and $f_{gb}= \pi\omega/\delta$, where ω is the grain boundary width, Equation(1.3) further demonstrates the important effect of grain refinement on superplasticity. A transformation occurs as grain size decreases, from lattice diffusion control to grain boundary diffusion control, and the strain rate $\dot{\epsilon}$ becomes proportional to δ^{-3} in Equation (1.2). Only high-angle boundaries would support such grain boundary diffusion. In general, diffusion-controlled grain boundary sliding is thought to be responsible for superplasticity and high-angle grain boundaries are necessary for this mechanism. However, complete details are not fully understood. [Ref. 3]

Commercial high-strength Al alloys are a result of alloy modification and processing to enhance their structural capabilities. These 'off the shelf' materials do not exhibit large tensile elongations or a superplastic response in the as-received condition. Thermomechanical processing (TMP) to

reduce grain size and alloy modifications for grain-size stabilization are important in attaining a superplastic response in these aluminum alloys.

Complex parts can be fabricated from a single piece of superplastic Al alloy at a pre-determined temperature strain-rate combination, minimizing the use of fasteners or welds which both increase the weight and decrease reliability. Fatigue and corrosion susceptibility are also reduced at joints and other critical stress concentrators by the forming of a single piece. Once formed, the superplastic material may be heat treated to restore mechanical properties. These advantages of superplastic materials are limited by economic factors. Existing commercial processes are slow due to low strain rates for superplastic response and this increases cost. High forming temperatures are also a problem. The development of a low-temperature, high strain-rate superplastic material would significantly advance the forming of components by this method.

By adjusting TMP schedules for an Al-Mg alloy, fine, stable grains were produced. Elongations exceeding 1000 pct. at a low temperature (T≈300°C) have been reported by workers at the Naval Postgraduate School (NPS) [Ref. 4]. Peak elongations were attained at strain rates of $10^{-3}s^{-1}$ and superplastic elongations were at strain rates of $10^{-1}s^{-1}$.

Superplastic response of the Al-Mg alloy is theorized to be due to microstructural grain refinement via particle-stimulated nucleation (PSN) of recrystallization during TMP [Ref. 5]. The observations of microstructure and superplastic response of the Al-Mg alloy prompted the search for a similar result in a high-strength commercial Al-Cu alloy. The Al-Cu phase diagram is similar to the Al-Mg diagram in that the Al-rich region exhibits a eutectic reaction involving an intermetallic phase and a terminal solid solution with appreciable solubility. Work on the Al-Cu alloy at NPS thus far has shown some superplasticity (≈260 pct.) at 450°C [Ref. 6]. The large average grain size(>10μm) in the Al-Cu alloy is believed to have limited the low temperature superplastic response.

This study attempted to identify and control critical parameters affecting grain size in the Al-Cu alloy 2519. The TMP schedules were adjusted based on PSN theory to control microstructure. Backscatter orientation contrast (BSOC) metallographic techniques were developed to improve the resolution of images over those obtained with optical microscopic methods. Image analysis measurement of BSOC micrographs were used to estimate a critical θ particle diameter, d_{crit}, for PSN of recrystallization. A method was developed to determine the effect of TMP on grain size.

II. BACKGROUND

A. ALUMINUM ALLOY PROPERTIES

Military requirements often dictate that components in platforms should have as high a strength to weight ratio as possible to give maximum advantage in range and payload. Aluminum alloys are light weight. Strengthening is accomplished via the following mechanisms.

1. Strengthening Mechanisms

Pure Al deforms by dislocation motion through the crystal lattice. By impeding dislocation motion, Al is strengthened [Ref. 2]. There are several strengthening mechanisms applicable to the 2519 Al-Cu alloy.

a. Solid Solution Strengthening

Substitutional and interstitial atoms distort the crystal lattice of a pure metal which results in stress fields that interfere with dislocation motion. The larger the size difference between pure Al and the alloying element, the larger the interaction stress field and resulting strength. Increasing the quantity of alloying element will increase the overall strength until the maximum solubility is exceeded. When this occurs, a different strengthening mechanism, dispersion strengthening is produced.

b. Precipitation Hardening

The temperature-dependent solubility of alloying elements, in which solubility decreases with decreasing temperature, provides the mechanism of precipitation hardening. Solution treatment above the solvus temperature to dissolve a second phase provides a homogenous single-phase solid solution. Rapidly quenching to room temperature produces an unstable supersaturated solid solution and, in the Al-Cu alloy, metastable GP zones and precipitates form at room temperature. At higher temperatures prolonged aging eventually results in the formation of the equilibrium θ (Al_2Cu) phase.

c. Strain Hardening

Plastic deformation generates large numbers of dislocations. Interactions among dislocations sliding on intersection slip planes reduce their mobility and increase the stress required to continue dislocation motion [Ref. 2], resulting in strain hardening.

2. Al-Cu 2519 Properties

The Al-Cu binary phase diagram is shown in Figure 2.1 [Ref. 7]. The Al rich eutectic region is similar to that for the Al-Mg alloys. The Al-Cu alloy 2519 has a Cu content

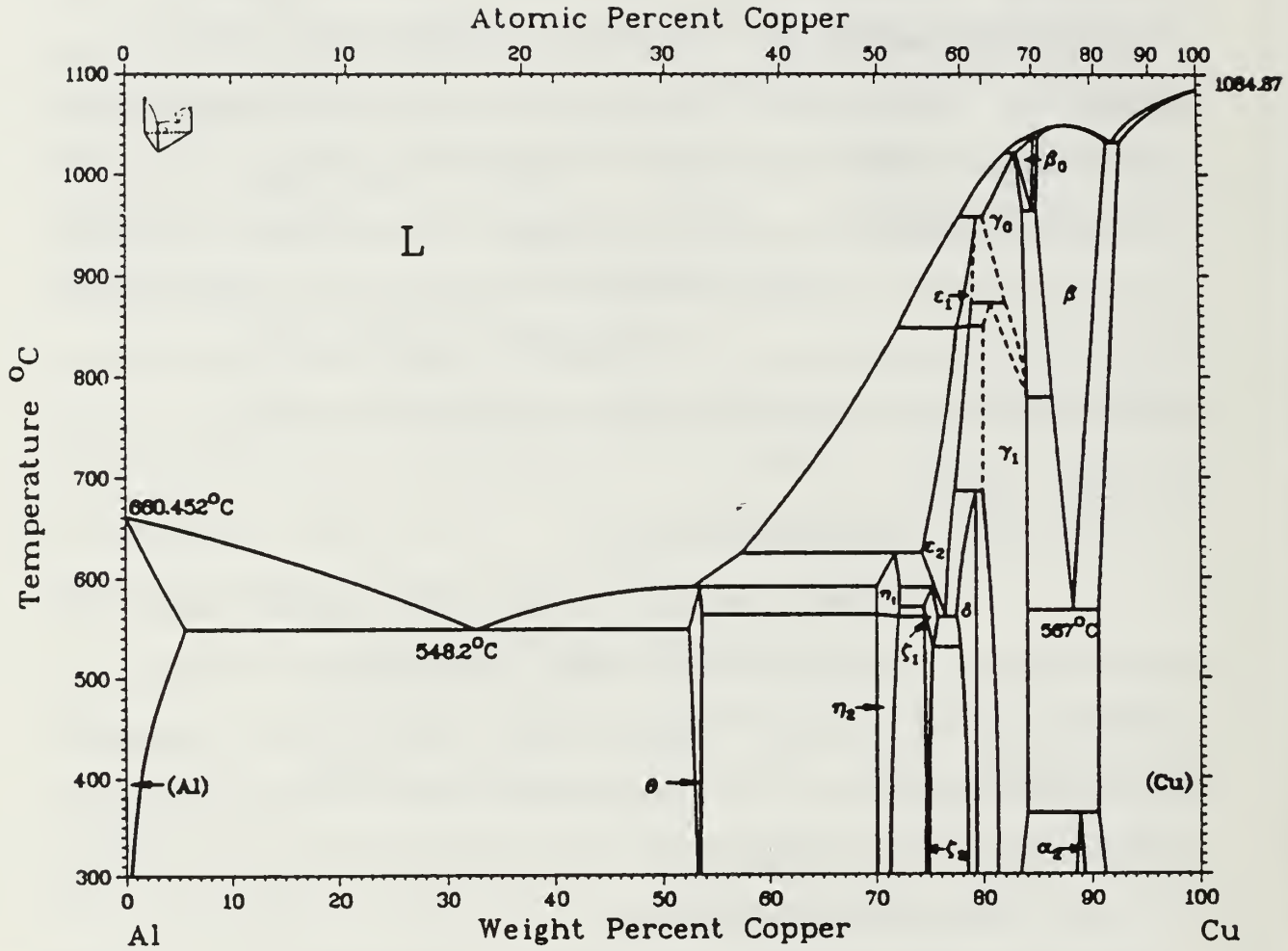

Figure 2.1. Al-Cu Phase Diagram [Ref. 7]

exceeding maximum solubility (5.65 wt. pct.); thus complete solution cannot occur, and some θ-phase particles remain undissolved throughout subsequent processing.

In the overaging of 2519 Al-Cu alloy, a continuous series of precipitates develop from the supersaturated solid solution. Precipitates develop sequentially either with increased temperature or increased time at temperature [Ref.8]. Precipitate structures are identified by the following notation:

$$\text{SSSS} \rightarrow \text{GP zones} \rightarrow (\theta)'' \rightarrow \theta' \rightarrow \theta$$

The initial aging process stage involves a transformation from random distribution of copper atoms changing to form disk-like planar aggregates in a supersaturated solid solution (SSSS) GP zones, and the intermediate phases θ'' and θ'. At elevated temperatures, the θ'-phase nucleates preferentially on dislocations. As time or temperature increases the θ' aggregates form a non-coherent θ phase. The θ size increases until the copper concentration reaches an equilibrium value in solution.

B. RECRYSTALLIZATION AND GRAIN SIZE

A fine and stable grain structure is crucial in obtaining a high m coefficient. There are two commercial methods to produce fine grains and superplasticity in Al alloys.

1. Commercial Methods

a. Rockwell Process

The Rockwell process [Ref.9] uses discontinuous recrystallization (DRX) to produce a refined grain structure capable of superplastic response. The thermomechanical processing (TMP) consists of four primary steps. The first step is a solution treatment to dissolve any precipitates in to solution. The second step is an overage which produces second-phase precipitate particles. Step three is extensive warm rolling that introduces strain energy in the form of dislocations to drive the subsequent recrystallization process. The final step is an recrystallization treatment in which new grains nucleate and grow. Grain refinement to $\approx 10\mu m$ is achieved by the Rockwell process [Ref. 9]. The DRX process apparently is strongly influenced by the size and distribution of second phase precipitate used to stimulate recrystallization. Precipitate particle were reported to be 0.5~1.0μm in size.

b. Supral Process

The principle of continuous recrystallization (CRX) is used in the Supral process to obtain a refined grain structure. An addition of 0.4 pct. Zr to an Al-6%Cu alloy, results in the formation of a fine dispersion of Al_3Zr

particles upon precipitation from solid solution. These fine precipitates help retard grain growth upon recrystallization during superplastic forming.[Ref. 10]

2. Particle Stimulated Nucleation (PSN) Theory

Dispersions of particles can assist in grain refinement if the individual particles become nucleation sites for recrystallization. PSN theory is based mainly on microstructural observations [Ref. 11]. Highly misoriented embryos may form within deformation zones near particles during plastic deformation [Ref. 12]. These substructures may also involve large dislocation densities and could become recrystallization nuclei and grow if certain criteria are met. The resulting theoretical relationships between strain and particle size may be exploited in TMP for grain refinement.

The requirement that a material move around a non-deforming particle to avoid the formation of interfacial voids can be achieved by local lattice rotations associated with introduction of geometrically necessary dislocations.[Ref.12] A model for the density of such dislocations, ρ_g, is given by [Ref. 13]

$$\rho_g = \frac{8f\gamma}{b\,d_p} \qquad (2.1)$$

where f is the volume fraction of particles, γ is the shear

strain, b is the Burger vector, and d_p is the particle diameter. The nature of the dislocation structure and how it effects PSN is based on particle diameter and strain [Ref.12]:

(a) Small particles (d_p<0.1μm) and low strains produce prismatic loops which do not provide lattice rotations (does not directly assist PSN);

(b) Large particles (d_p>0.1μm) and larger strains result in dislocations that produce local lattice rotations near the particles (required for PSN).

PSN has been observed mostly at particles ≥ 1.0μm suggesting that local lattice rotation is not the only prerequisite for nucleation.

Within a deformation zone, local lattice rotations form highly misoriented structures termed embryos. One or more of the embryos may form a recrystallized grain. The energy for growth of such an embryonic grain is the second consideration for PSN. A nucleus capable of growth must exceed a critical diameter , δ_{crit} in order to expand into the surrounding matrix [Ref. 12,14]:

$$\delta_{crit} = \frac{4\Gamma}{E} \qquad (2.2)$$

where Γ is the grain boundary interfacial energy and E is the stored strain energy due to deformation. For nucleation to occur, a second criterion must be met: $\delta_{crit}<\lambda$. The size of the deformation zone ,λ, is estimated from continuum models [Ref. 15]

$$\lambda = A d_p \epsilon^{\left(\frac{n}{n+1}\right)} \tag{2.3}$$

where A is a material constant, d_p is particle diameter and n is the exponent from the strain hardening law ($\sigma=K\epsilon^n$). The corresponding free energy of formation, ΔG*, of the nucleus is given by

$$\Delta G^* = \frac{16\pi\Gamma^3}{3E^2} \tag{2.4}$$

For nucleation to occur at an appreciable rate, ΔG^* must be sufficiently small compared to kT. The following two considerations can be established: (1) increased d_p and/or ϵ increases λ; (2) larger λ increases the number of particles at which embryonic grains that may satisfy $\delta_{crit}\leq\lambda$, thus increasing the possible number of grains. The relationship between d_p and ϵ for PSN is illustrated schematically in Figure 2.2. According to this theory, the strain must exceed

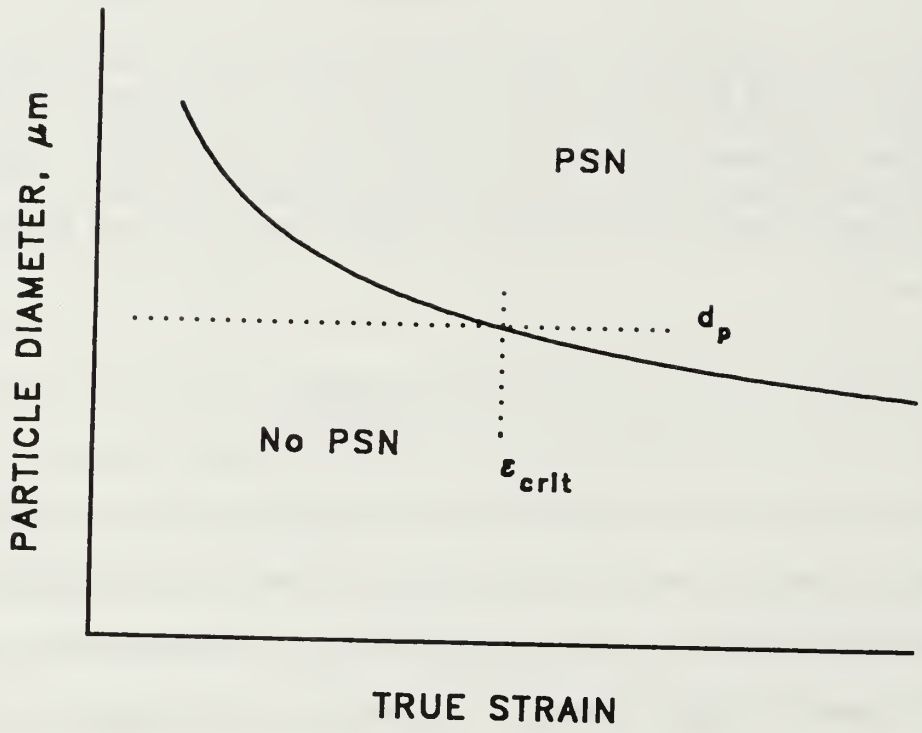

Figure 2.2. Relationship between Particle Diameter and Strain for Particle Stimulated Nucleation.

a value ϵ_{crit} in order to initiate PSN in a material with a particle size d_p. Smaller particle size requires increased strain to induce PSN.

3. Grain Size

An estimate of grain size can be made if it is assumed that all grains nucleated grow only until they contact each other. An approximation of grain size, δ, can be made if essentially all θ particles are assumed to have size $\geq d_{crit}$ and nucleate grains via PSN then,

$$\delta \approx D_s \approx \frac{d_p}{f^{\frac{1}{3}}} \qquad (2.5)$$

where D_s is the θ particle spacing.

C. GRAIN REFINEMENT TECHNIQUES

Low temperature superplastic response has been attained in Al-Mg alloys for appropriate combinations of TMP variables [Ref. 16]. These TMP schedules consisted of initial solution treatment and hot working (by upset forging) at the same temperature. Following quenching the material was reheated for warm rolling at 300°C. Warm rolling is accomplished by a series of reductions with inter-pass anneals (IPA). Large superplastic elongations were achieved by a process including

lengthy 30 minute IPAs. Reported results using BSOC have shown microstructural grain refinement via PSN associated with β-phase (Al_8Mg_5) precipitates. The prolonged IPA facilitated precipitation and coarsening the β phase and also formation of recovered structures prior to the onset of PSN. Recrystallization via PSN was achieved with β-particles of 0.85μm average size.

Mathé [Ref. 17] studied overaging of the 2519 Al-Cu alloy to determine conditions required for formation of θ particles $\approx$1.0 μm in size. A pre-strain of 10 pct. at 200°C and overaging at 450°C for 10 hours resulted in many particles $\approx$1-2μm in size. Particles of this range were estimated to be within d_{crit} for PSN based on Al-Mg results. However, a grain size >10 μm was produced which did not exhibit superplasticity (<160 pct. elongation). Bohman [Ref. 6] subsequently made further TMP modifications based on PSN theory in an attempt to reduce grain size. Process parameters such as rolling temperature, overaging time and IPA time were adjusted but with minimal grain size reduction. Bohman's TMP D resulted in the largest superplastic response of 260 pct. elongation. The current study was initiated to further study effects of process parameters and obtain quantitative information on the particle size and size distribution in relation to recrystallization in this alloy.

D. BACKSCATTER ORIENTATION-CONTRAST (BSOC)

Resolution improvements beyond optical methods were necessary for an analysis of the particles as well as grain refinement. The Transmission Electron Microscope (TEM), with the highest resolution available, was not considered. Thin foil preparation precluded its use since few large θ particles in the 2519 Al-Cu alloy are likely to be present in the thin region of a foil and an excessive number of foils might be required for acceptable statistical analysis. The scanning electron microscope (SEM) can provide resolutions down to 20Å, which is a vast improvement over optical resolutions of 3000-5000Å. However previous SEM work on 2519 Al-Cu encountered low orientation-contrast intensities in the backscatter mode which limited its application.

The SEM Backscatter Detection (BSD) detects incident electrons that strike the surface and are back-scattered toward a Li-drifted Si crystal detector. There are two important sources of contrast due to these electrons. The first and most widely used is the contrast due to atomic number differences. Back-scattered images are very sensitive to atomic number differences. Elements of large atomic number are more efficient in elastic scattering of electrons and regions containing high concentrations of such elements appear brighter due to the large quantities of electrons reaching the

detector. Elements of small atomic number are less efficient at back-scattering, and regions with such elements appear darker in contrast. In the 2519 Al-Cu alloy, the θ precipitates are light in contrast due to the large average atomic number of Al_2Cu when compared to the surrounding Al matrix. Difficulties arise when a lower intensity type of contrast, such as backscatter orientation-contrast(BSOC) are desired.

From Rutherford backscattering, a relationship between BSOC intensity, I, and electron accelerating voltage, E_o , can be used to increase detection levels of weak signals:

$$I \propto I_o(\frac{eZ}{4E_o})^2 \qquad (2.6)$$

where I_o is the incident intensity, e is the electronic charge, and Z is atomic number.

At a lower accelerating voltage, the total back-scattered intensity will be reduced as I_o will decrease. The ratio of intensities due to the atomic number difference will be the same at the lower voltage (Equation (2.6)) but the difference in intensities due to orientation as well as atomic number effects will be reduced and thereby fall within the operating range of the detector. In effect, an equalization occurs between atomic number intensity and orientation-contrast intensity as E_o decreases. Normal accelerating voltages of 20

KV show a dark matrix with only light θ particles. Reducing the acceleration voltage to 5KV allowed both the θ and orientation contrast to be seen on the same micrograph.

III. EXPERIMENTAL PROCEDURE

A. MATERIAL

The 2519 Al-Cu alloy studied was provided by ALCOA Technical center. The as-received material was in the form of a rolled plate in the T87 temper condition. This condition corresponds to solution treating at 535°C, cold rolling to 7 pct. strain, and artificial aging 24 hours at 165°C [Ref.18]. The composition of the material is provided in Table 3.1.

TABLE 3.1 COMPOSITION OF Al-2519 (WEIGHT PERCENT)

Cu	Mn	Mg	Fe	Zr	V	Si	Ti	Zn	Ni	Be	B	Al
6.06	0.30	0.21	0.16	0.13	0.04	0.07	0.06	0.03	0.01	.002	.001	bal

Values listed are within the limits specified in the Metals Handbook [Ref. 19].

Billets measuring 61.0 x 38.1 x 22.2 mm were sectioned from the as-received plate. These billets were cut with the greatest dimension parallel to the rolling direction of the as-received plate.

B. PROCESSING

All TMPs used employed four major steps, consisting of: (1) solution treatment; (2) pre-strain; (3) overaging; and (4) rolling with a controlled IPA time. Figure 3.1 illustrates the various TMP schedules examined.

1. Solution Treatment and Pre-strain

Solution treatment was performed in a Lindberg Furnace, Model 51828, by heating at 535°C for 100 minutes. A room-temperature water quench results in a super saturated solid solution after which a pre-strain of 10 pct. (5pct. in each of two passes) at 200°C was introduced to provide sufficient dislocations to serve as nucleation sites for θ' precipitation. For the Cu content of this alloy (≈6 wt. pct.), the metastable θ' solvous temperature is just above 450°C [Ref. 20]

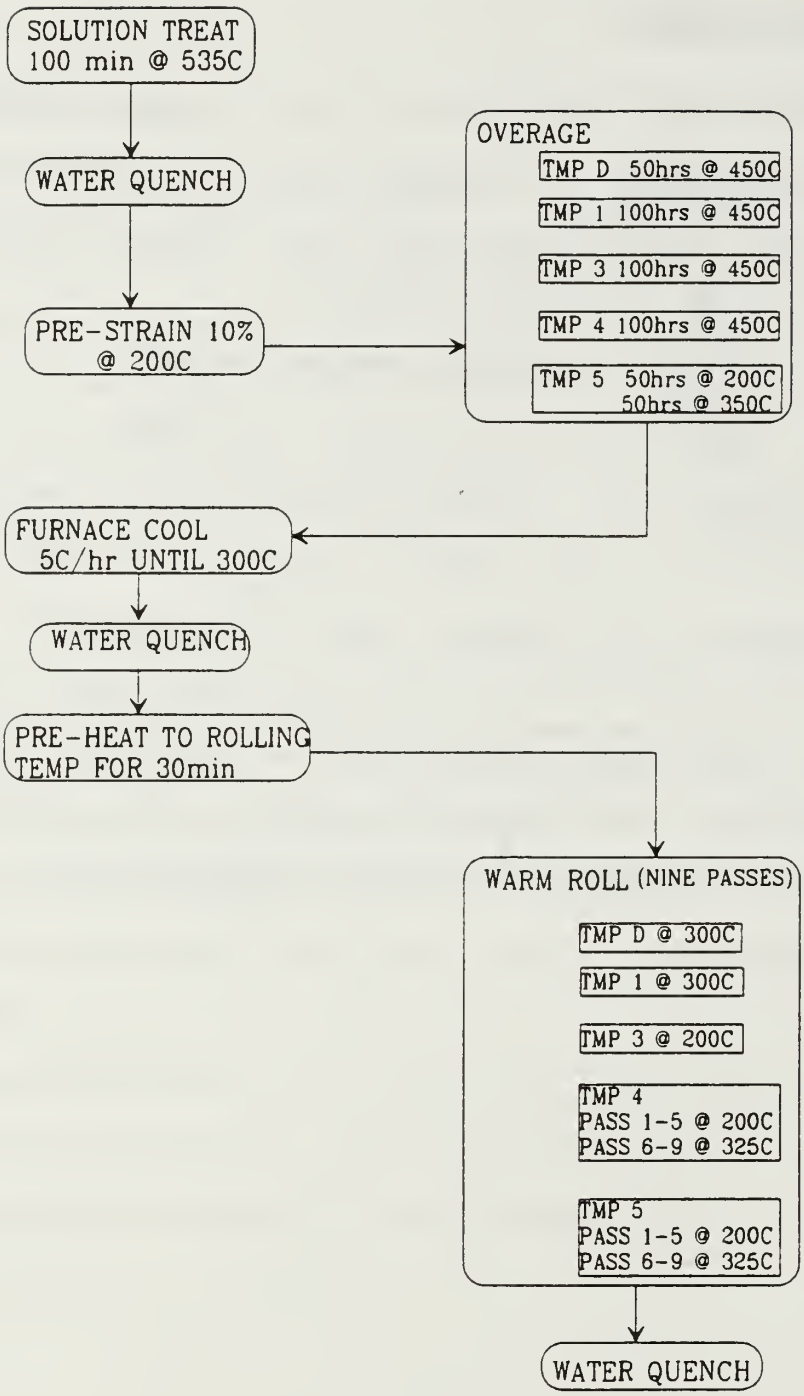

Figure 3.1. Schematic Representation of TMPs Investigated

2. Overaging

Following the pre-strain, the billets were overaged at 450°C for either 50 or 100 hours. The exception was the TMP 5 condition in which overaging at 200°C for 50 hours was followed by further overaging at 350°C for an additional 50 hours. By overaging at 200°C for 50 hours, the θ'-phase formed initially is anticipated to transform to θ -phase. The effect of the pre-strain on homogenizing the ultimate distribution of the θ-phase is thereby improved. The goal of the overaging process was to provide a θ precipitate size distribution with a large fraction of particles above d_{crit} for PSN.

3. Warm Rolling

A pre-heat for 30 minutes at the rolling temperature ensured no transients were present providing for a uniform starting condition. The rolling portion of the TMP consisted of nine reduction passes of increasing strain and strain rate on each successive pass. An IPA of 30 minutes at the rolling temperature was used reflecting previous work on the Al-Mg alloys. After the final pass, the material was quenched to room temperature. Samples were sectioned from the rolled material for subsequent annealing and microscopic analysis. The rolling was conducted on a Fenn Laboratory mill with a roll diameter of 4.0 inches and rotation at 0.327

radian/second. The true strain, ϵ_{pass}, and strain rate, $\dot{\epsilon}_{pass}$, for each pass were calculated from Equations (3.1 and 3.2) as:

$$\epsilon_{pass} = \ln\left(\frac{t_i}{t_f}\right) \tag{3.1}$$

and

$$\dot{\epsilon} = \frac{2\pi Rn}{\sqrt{Rt_i}}\sqrt{\epsilon\left(1+\frac{\epsilon}{4}\right)} \tag{3.2}$$

where t_i is the material initial thickness, t_f is the rolling mill gap setting, R is the radius of the roller (inches), and n is the rotational speed of the rolls (radian/second). Table 3.2 provides a summary of the TMP reduction schedule.

TABLE 3.2 ROLLING SCHEDULE

ROLL PASS	INITIAL THICKNESS (in)	MILL GAP SETTING (in)	RESULTING THICKNESS (in)	MILL DEFLECT (in)	TRUE STRAIN (pct.)	STRAIN RATE (1/s)
1	0.826	0.742	0.763	0.021	10.72	1.075
2	0.763	0.657	0.678	0.021	14.95	1.335
3	0.678	0.581	0.603	0.022	15.39	1.440
4	0.603	0.531	0.532	0.001	12.72	1.377
5	0.532	0.431	0.459	0.028	21.05	1.924
6	0.459	0.338	0.365	0.027	30.60	2.554
7	0.365	0.227	0.255	0.028	47.49	3.708
8	0.255	0.123	0.156	0.033	72.91	5.808
9	0.156	0.045	0.084	0.039	124.32	10.752

C. SAMPLE PREPARATION

1. Grinding

The transverse-longitudinal (T-L) surfaces of the as-rolled and annealed samples were prepared for SEM examination. The samples were prepared by cutting to size ($\approx 1 cm^2$) with a SBT-Model 650 low speed diamond saw. The T-L surface was ground un-mounted on wet-dry sandpaper using standard techniques.

2. Mechanical Polishing

Each sample was polished using 6μm and 1μm diamond compound. Variable-speed twelve inch polishing wheels were set to 220 rpm. The polishing sample was moved in a clockwise direction applying light pressure. Polishing continued until the surface was mirror like with no visible 6μm scratches.

3. Electropolishing

A solution of 70 pct. Methanal and 30 pct. Nitric acid, maintained at -20°C in a Methanol bath, was used for electropolishing. A voltage of 4-6 VDC was applied for 2 minutes, resulting in an average current density of 0.08 amps/cm^2. After electropolishing, the sample was rinsed in clean Methanol. Several sources of contamination can obscure the backscatter electron image. First, the insulating resin must be completely dry on the sample prior to electropolishing. Second, the Methanol rinse stream after polishing is complete should be perpendicular to the electropolished surface. Third, the clean Methanol for post-polish rinse should be stored in a glass container rather than polyethylene bottles. Other wise, residues may form on polished samples.

D. SCANNING ELECTRON MICROSCOPY

A Cambridge model S200 SEM equipped with a tungsten filament was used in the backscatter mode at a low accelerating voltage in order to reveal orientation contrast images.

E. IMAGE ANALYSIS

Image analysis was performed to characterize both the grain size and the θ particles. The Image-Pro (IP) II Image Processing System, Version 2.0, and the Microscience ImageMeasure system were utilized. Length was measured by the maximum length of a chord rotated through 180° within the object. The maximum chord length method used by IP differs from the conventional (non-digital) mean intercept method. Many reported results in superplastic research have been obtained using mean intercept method. A conversion factor relating the maximum cord and mean intercept method can only be approximated. Area is based on the number of pixels interior to and under an object boundary. Data was generated tabularly and exported into Sigma Plot software for histogram generation.

IV. RESULTS AND DISCUSSION

A. TMP MODIFICATIONS AND MICROSTRUCTURE

Prior work on 2519 Al-Cu alloy involved adjusting TMP parameters and evaluating subsequent superplastic response by mechanical testing. Refinement to grain size of ≈ 10μm was reported. It became apparent, however, that the 2519 Al-Cu alloy was grain refined to a lesser extent than achieved with the Al-Mg alloy by the same TMP. Bohman [Ref. 6] recommended that his TMP D (best superplastic response) be modified by increasing the overaging time and reducing rolling temperature. The TMP variables selected for investigation in this research are based on this recommendation and are summarized in Table 4.1.

TABLE 4.1 TMP SCHEDULES INVESTIGATED

	TMP D	TMP 1	TMP 3	TMP 4	TMP 5
OVERAGE TIME	50 hr @450°C	100 hr @450°C	100 hr @450°C	100 hr @450°C	50 hr @200°C 50 hr @ 350°C
WARM ROLL TEMP	300°C	300°C	200°C	PASS 1-5 200°C PASS 6-9 325°C	PASS 1-5 200°C PASS 6-9 325°C

In the first phase of this study (TMP 1), overaging time was increased from 50 to 100 hours. By increasing the overaging time, the time available for precipitation and coarsening of θ particles was increased. It was anticipated that more numerous large θ particles would increase the number of nucleation sites and thereby reduce the resulting grain size.

The second process (TMP 3) examined the effect of rolling temperature on PSN. The rolling temperature was reduced from 300°C to 200°C to increase stored strain energy. Phase three (TMP 4) consisted of adjusting IPA and rolling temperatures between pass six through nine to 325°C. This process represents conditions similar to those in the latter stages of the processing of the Al-Mg alloys.

The final phase (TMP 5) altered the overage process to include a two-step procedure. Step one, a 50 hour overage at 200°C, was intended to allow θ' to precipitate at dislocations and transform to θ at this low temperature. Step two, a 50 hour overage at 350°C, was to coarsen this θ phase and retain the benefits of the initial pre-strain to a greater extent.

1. Microscopy Results

A typical backscatter micrograph of TMP 4 shows a homogenous dispersion of θ particles (Figure 4.1(a)). When backscatter orientation-contrast (BSOC) effects are enhanced, the as-rolled un-recrystallized structure becomes visible along with the θ particles (Figure 4.1(b)). The apparent formation of recrystallized grains occurred at a post rolling anneal of ≈ 325°C for 10 minutes. Once recrystallized, grains appeared stable over the temperature/time range tested as summarized for TMP 3 in Table 4.2.

TABLE 4.2 TMP 3 GRAIN SIZE DATA

TMP 3 ANNEAL	LENGTH (μM)	AREA (μM^2)
(325°C/30MIN)	12.1	66.9
(375°C/10MIN)	12.5	73.6
(375°C/30MIN)	12.8	74.6
(450°C/5MIN)	13.5	78.7

A low recrystallization temperature of 375°C for 10 minutes was chosen as the standard condition to compare TMP effects. After recrystallization at the standard condition, BSOC mode reveals an equiaxed, apparently recrystallized grain structure (Figure 4.1 (c)).

(a)

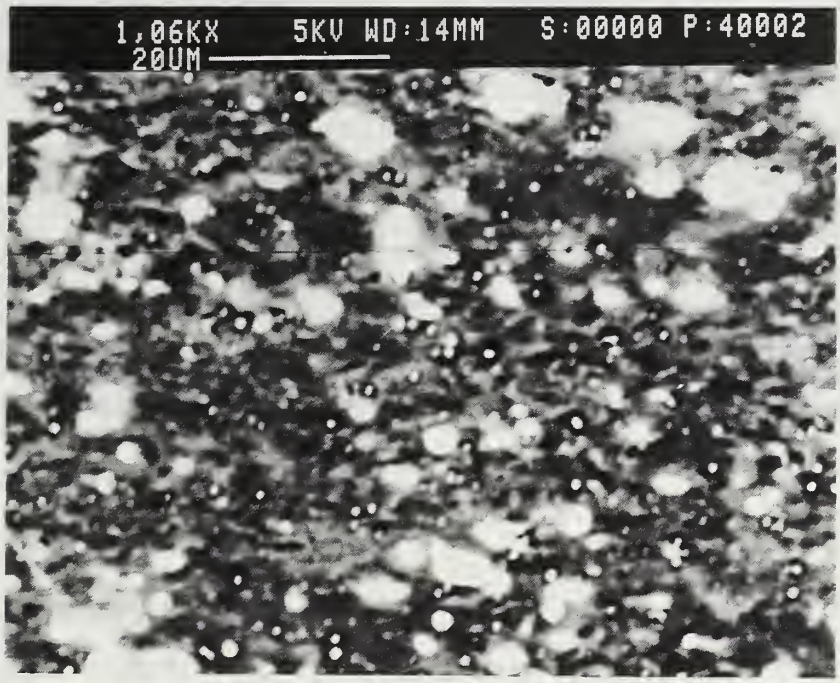

(b)

Figure 4.1. Backscattered electron micrographs showing the 2519 Al-Cu alloy processed by TMP 4: a) atomic number contrast; b) enhanced orientation-contrast; (continued)

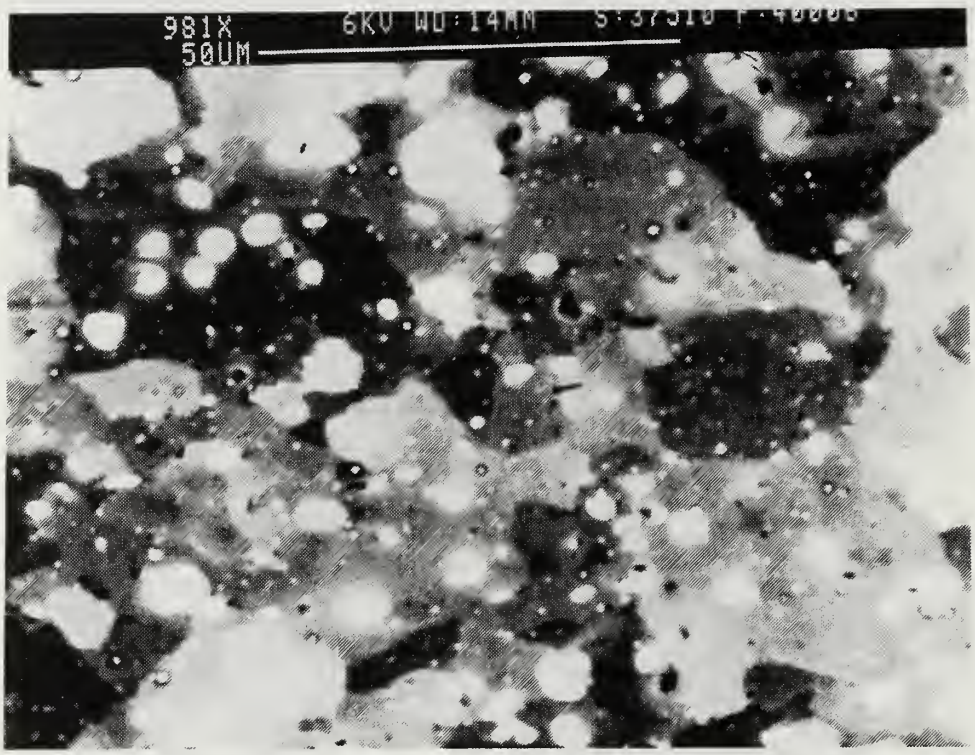

(c)

Figure 4.1. c)annealed (375°C/10min). Enhanced orientation contrast indicates recrystallized grain structure.

Many variables effected the contrast and sharpness in the backscatter orientation-contrast (BSOC) method. To attempt to quantify these would be misleading since no consistent setting gave the best images. The following settings provided an initial starting point:

(a) Accelerating voltage at 5KV

(b) Spot size at setting 5

(c) Working distance at 14 mm

(d) Backscatter unit set on high contrast

Three controls affected orientation contrast: backscatter brightness control, backscatter contrast control, and the SEM fine probe control. Best images were obtained when these controls were adjusted concurrently.

A low accelerating voltage in the BSOC mode created a focus problem due to decreasing electron wave length which limited magnification to ≈1200X. Gun alignment had to be accomplished at the voltage and spot size used in BSOC in order to obtain the sharpest image.

2. Effects of Overageing

TMP 1 examined the effect of increasing the overaging time compared to that of Bohman's work [Ref. 6] in an attempt to increase the quantity of larger θ precipitates. Based on the PSN model, the greater the number of θ precipitates above d_{crit} the greater number of nucleation sites.

Image analysis of both TMP D and TMP 1 revealed θ-particle length measurements indicating a similar size and distribution of these particles. (Figures 4.2(a) and 4.2(b)). TMP 1 showed no apparent distribution shift in grain size of statistical significance (Figures 4.3(a) and 4.3(b)) compared to TMP D.

3. Effect of Rolling Temperature

TMP 3 examined the effect of decreasing rolling temperature. Reduced rolling temperature increases the stored strain energy which should reduce d_{crit} for PSN. Rolling temperature was decreased to 200°C. Figure 4.2(c) shows the distribution of the θ particle size is similar to the previous distributions while Figure 4.3(c) shows no significant shift in grain size from previous measurements.

4. Effect of Substructure on Recrystalization

The Al-Mg alloy had displayed sub-grain formation during reheating intervals between passes prior to the onset of recrystallization in the final stages. The 2519 Al-Cu TMP 4 was modified for pass 6 through 9 to incorporate subgrain formation. The temperature selected was 325°C, at which recrystallization had occurred in post TMP anneals previously. The TMP 4 grain size data shown on Figure 4.3(d) is similar to those of previous TMP's. The θ particle distribution, Figure 4.2(d), is also similar to those of previous processes suggesting that the anneals had no effect.

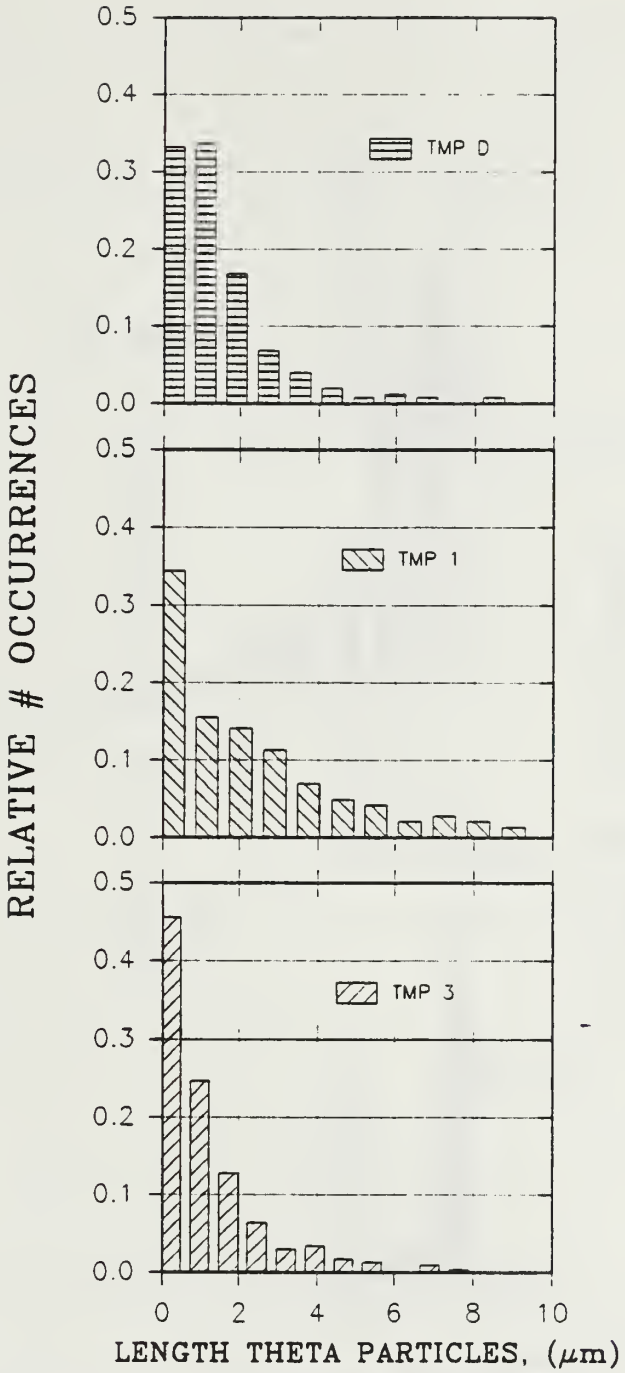

Figure 4.2. **Normalized θ Particle length Distribution Measurements: a) TMP D; b) TMP 1; c) TMP 3; (continued)**

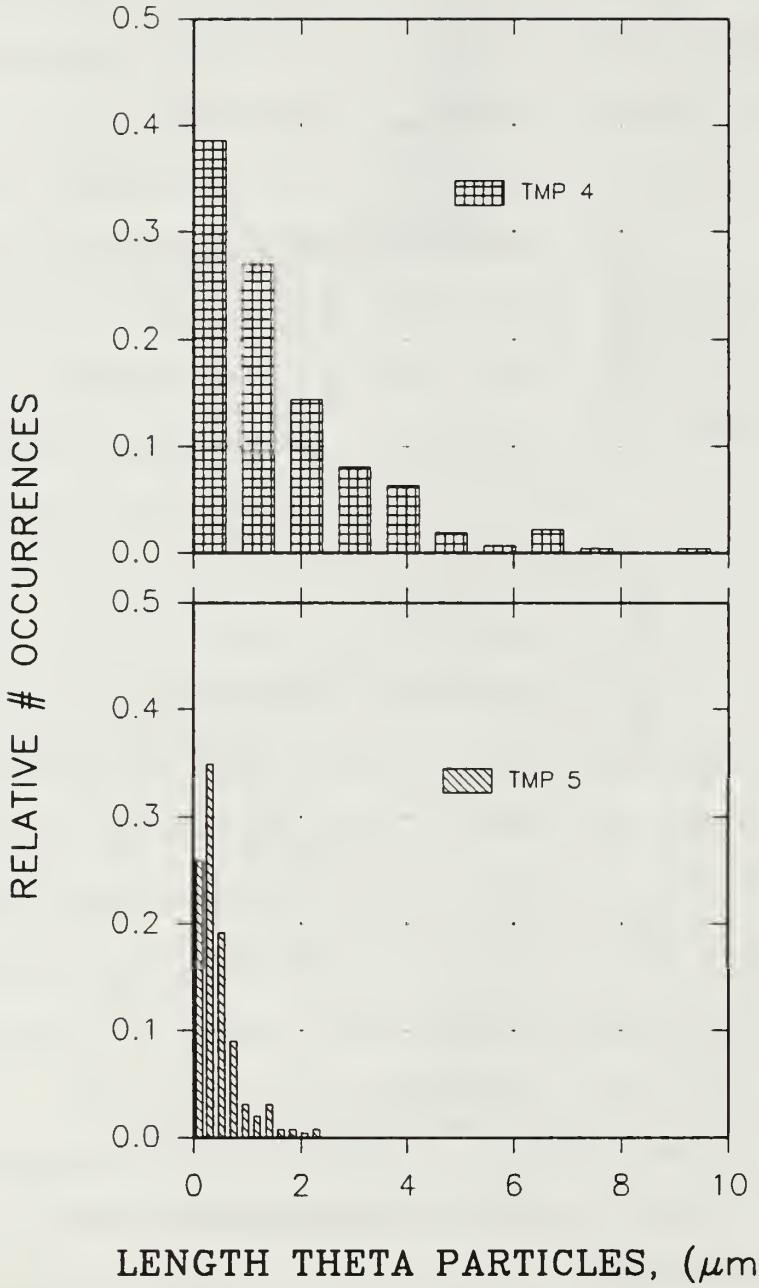

Figure 4.2. **c) TMP 4; d) TMP 5.**

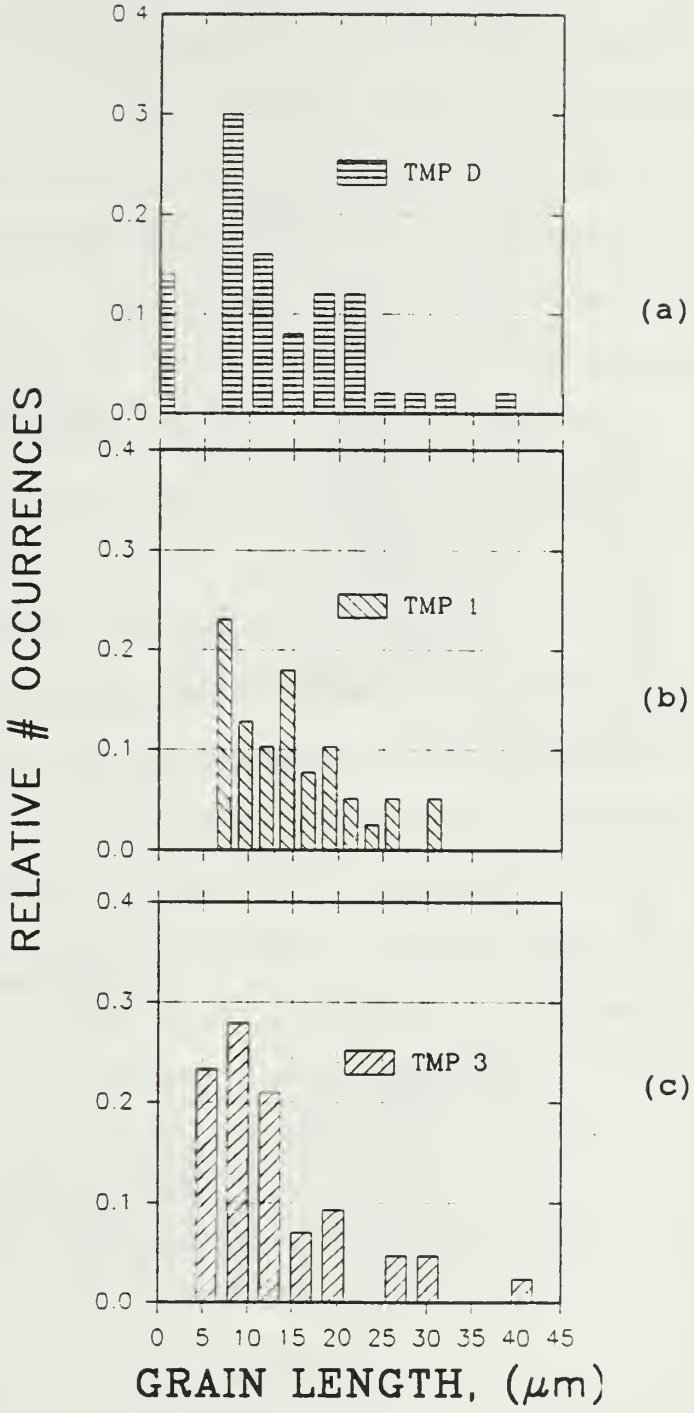

Figure 4.3. Normalized Grain Size Distribution Measurements: a) TMP D; b) TMP 1; c) TMP 3; (continued)

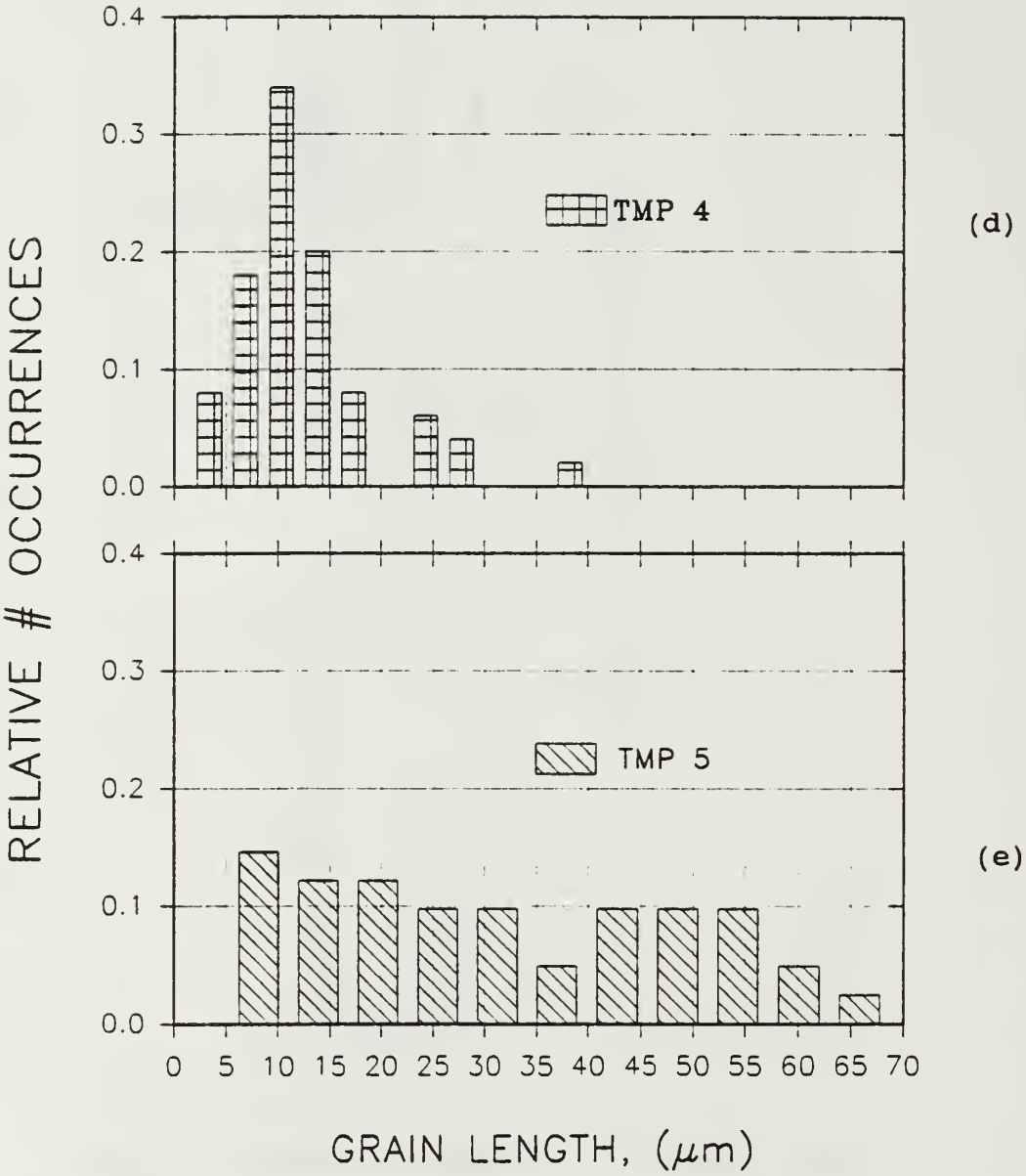

Figure 4.3. **c) TMP 4; d) TMP 5.**

The data on particle and grain size of the examined TMP's suggests that none of the process modifications were successful in grain refinement. An approximate calculation of the critical θ particle size, d_{crit}, for PSN was obtained and is described later in this thesis. Essentially, the θ particle size distributions examined were below d_{crit} and process variations influenced mainly these smaller particles. A narrow distribution centered near d_{crit} was the desired effect of the next TMP modification.

5. Effect of Two Step Overage

Step one in the overage (50 hours at 200°C) was to intended to allow the θ' to precipitate on dislocations and then to transform to θ at this lower temperature. This would provide a more homogenous dispersion since θ tends to precipitate at prior boundaries at higher temperatures. Step two (50 hours at 350°C) was then intended to coarsen the resultant θ particles and achieve a size above d_{crit}.

The resulting θ particle distribution is shown in the backscatter image of Figure 4.4(a) and the corresponding BSOC micrograph in Figure 4.4(b) illustrates the grain size obtained in subsequent processing. The θ particles are clearly finer than those produced at higher overaging temperature (compare Figures 4.1(a) and 4.4(a) and note the 3X magnification difference). The histogram of Figure 4.2(e) also reveals the fine distribution of θ particles. In association with these much finer particles, the grain size is much coarser (compare Figure 4.1(c) to 4.4(b)). These results suggest that this treatment has actually reduced the number of particles of size $\geq d_{crit}$ for PSN. Comparison of the histograms of Figure 4.2 and the grain size data suggest that d_{crit} is likely 2.0μm or greater (above the range for TMP 5) for all of the rolling conditions examined.

B. QUANTITATIVE ANALYSIS

The estimation of a critical particle size for PSN, from the results obtained here, would provide future direction in judging the necessary change in particle size distribution and also guide the modification of the TMP schedules.

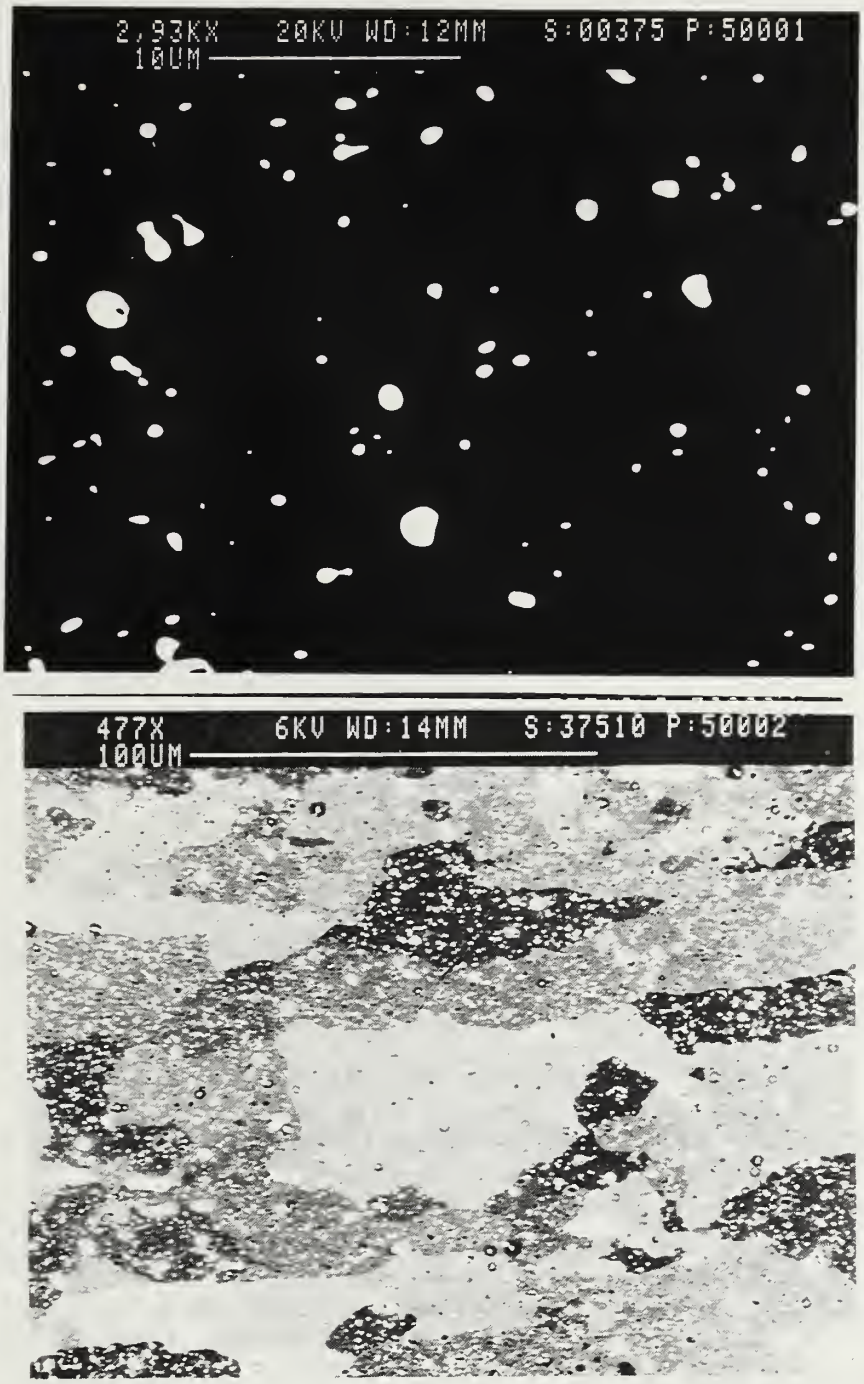

Fig 4.4. Backscattered electron micrographs showing the 2519 Al-Cu alloy processed by TMP 5: a) atomic number contrast; b) annealed (375°C/10min) enhanced orientation-contrast.

The Image-Pro (IP) software digitized the backscatter micrographs and measured the θ particle and apparent grain size. Analysis of the θ particle distribution allowed for an approximation of a critical diameter, d_{crit}, to be expressed for PSN.

From within a window area defined by the user, A_W, measurement and statistical data was calculated by IP. A total θ particle area contained in window, $A_{\theta,T}$, was calculated by IP. The θ particle fraction , f, is determined by:

$$f = \frac{V_{\theta,T}}{V_W} = \frac{A_{\theta,T}}{A_W} \qquad (4.1)$$

where $V_{\theta,T}$ is the total volume of θ particles, and V_W is the total alloy volume. If the θ particles are assumed to be spherical

$$V_{\theta,T} = \sum_i \left(\frac{\pi}{4} d_{p,i}^{\,3} * N_{p,i}\right) \qquad (4.2)$$

where $d_{p,i}$ is the mean particle size of the ith size class and $N_{p,i}$ is the number of particles in the ith class. From Equations (4.1 and 4.2):

$$V_W = \frac{V_{\theta,T}}{f} = [\sum_i (\frac{\pi}{4} d_{p,i}{}^3 * N_{p,i})] \frac{A_W}{A_{\theta,T}} \qquad (4.3)$$

A mean grain size is calculated by IP and may be used to provide the particle spacing, D_s, of particles capable of nucleating recrystallization. This assumes that grains will grow only until they touch and that no grains are lost, i.e., nucleation is site-saturated. Grain volume is estimated by assuming spherical grain shape. The number of grains per unit volume can then be calculated as:

$$N_G = \frac{V_W}{\frac{\pi}{4} D_s^3} \qquad (4.4)$$

From the θ particle size distribution histogram, starting at the largest particle class, the number of occurrences associated with each class are counted until $\geq N_G$. The mean particle size associated with the final class counted is the assumed to represent the critical diameter for PSN. Table 4.3 summarizes the estimates of d_{crit} for TMP conditions examined according to this procedure.

TABLE 4.3 CRITICAL PARTICLE SIZE

	d_{crit}
TMP D	2.7
TMP 1	3.8
TMP 4	3.0
TMP 3	2.5
TMP 5	-----

Note: TMP 5 CRITICAL DIAMETER ≈ TMP 4 (SIMILAR PROCESS)

The relation of the d_{crit} value estimated in this manner to the corresponding particle size distributions is illustrated schematically in Figure 4.5. From this, it appears that the process modification attempted thus far have not greatly affected the number of particles of size ≥ d_{crit} except in the case of TMP 5.

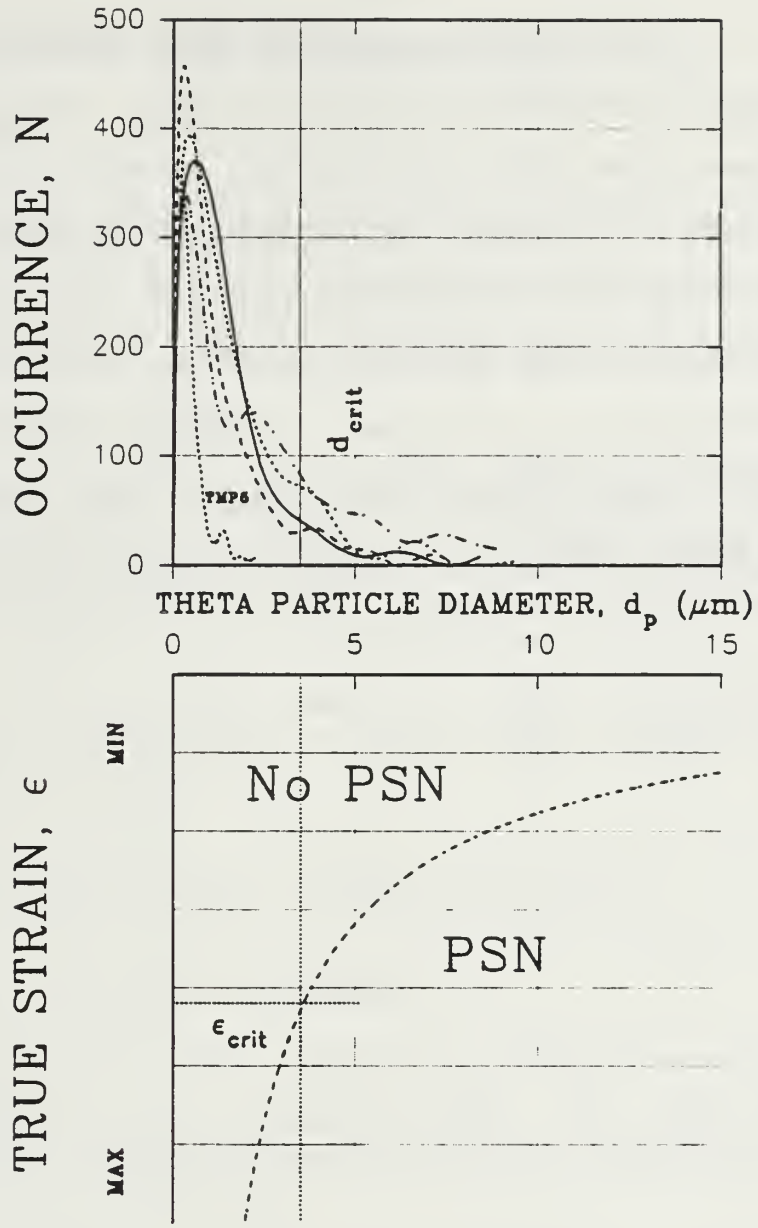

Figure 4.5. **Comparison of measured particle size distribution and a typical estimated d_{crit} value with a schematic representation of the condition for Particle Stimulated Nucleation.**

It is recognized that this estimation procedure is subject to several sources of error. Nevertheless, the data suggest that the combinations of TMP's D, 1, 3 and 4 all achieve recrystallization only at particles in the upper "tail" of the size distribution and that attempts to coarsen particles likely affected only the smaller particles in the distribution. To attempt to reduce the distribution width (TMP 5) was successful but the mean size was shifted downward and away from values sufficient for PSN (Figure 4.5).

V. CONCLUSIONS AND RECOMMENDATIONS

A. CONCLUSIONS

A variety of thermomechanical processing techniques have been employed and methods developed to determine the resultant effect on grain refinement. The conclusions and observations of this research are as follows:

1. Backscatter orientation-contrast (BSOC) microscopy techniques were developed and provided both grain-orientation and θ-phase precipitate contrasts on the same micrograph. Reduced accelerating voltage to 5KV is believed to have increased orientation-contrast beyond a threshold detection level.

2. Image analysis measurements of BSOC micrographs assisted in estimating an approximate critical θ-precipitate diameter, d_{crit}, for PSN of recrystallization.

3. Increased overaging time from 50 hours to 100 hours at 450°C had no effect in grain refinement.

4. Decreasing TMP warm rolling from 300°C to 200°C had no effect on grain refinement.

5. TMP 5, with a two step overaging, produced a narrow distribution of θ precipitates but was not sufficient in size capable of PSN. An increased second step overaging temperature may coarsen the θ precipitates toward d_{crit}.

6. TMP 5 produced a course grain structure of $\approx 30\mu m$ apparently due to $\theta < d_{crit}$.

B. RECOMMENDATIONS

The recommendations for further research are as follows:

1. Modify TMP 5's second overage temperature from 350°C to 450°C and determine coarsening effect.

2. Eliminate inter-pass anneals from pass 5 through 9.

LIST OF REFERENCES

1. Pilling, J., and Ridley, N., *Superplasticity in Crystalline Solids*, The Institute of Metals, 1989.

2. Meyers, M.A., and Chawla, K.K., *Mechanical Metallurgy Principles and Applications*, Prentice-Hall, Inc., 1984.

3. Sherby, O.D., and Wadsworth, J., "Development and Characterization of Fine-Grain Superplastic Materials," Deformation, Processing and Structure, *American Society for Metals*, 1982.

4. Hales, S.J., McNelley, T.R., and McQueen, H.J., "Recrystallization and Superplasticity at 300°C in an Aluminum-Magnesium Alloy," *Metallurgical Transactions* A, Vol. 22A, pp. 1037-1047, May 1991.

5. Crooks, R., Kalu, P.N., and McNelley, T.R., "Use of Backscattered Electron Imaging to Characterize Microstructure of a Superplastic Al-10Mg-0.1Zr Alloy," *Scripta Metallurgica*, Vol. 25, pp. 1321-1325, 1991.

6. Bohman, S.D., *Thermomechanical Processing of Aluminum Alloy 2519 for Grain Refinement and Superplasticity*,Master's Thesis, Naval Postgraduate School, Monterey, CA, June 1992.

7. "Binary Alloy Phase Diagrams," *American Society for Metals*, Vol. 1, Metals Park, Ohio, 1986.

8. *ASM Handbook*, American Society for Metals, 10th ed., Vol.4, pp. 823-880, 1991.

9. Wert, J.A., "Grain Refinement and Grain Size Control," *Superplastic Aluminum Alloys*, edited by Paton, N.E., and Hamilton, C.H., pp.69-83, Conference proceedings, TMS-AIME, Warrendale, PA, 1982.

10. Watts, B.M., Stowell, M.J., Baikie, B.L., and Owen, D.G.E., "Superplasticity in Al-Cu-Zr Alloys, Part II: Microstructural Study," *Metal Science Journal*, Vol. 10, No. 6, pp. 189-197, 1976.

11. Humphreys, F.J., "Nucleation of Recrystallization in Metals and Alloys with Large Particles," *1st Riso International Symposium (Denmark)*, pp.35, 1980.

12. Humphreys, F.J., "Local Lattice Rotations at Second Phase Particles in Deformed Metals," *Scripta Metallurgica*, Vol.27, pp. 1801-1814, 1979.

13. Ashby, M.F., *Philos. Metall.*, 21 (1970) 399.

14. Humphreys, F.J., *Acta. Metall.*, 25 (1977) 1323.

15. Argon, A.S., Im, J. and Safoglu, R., "Cavity Formation From Inclusions in Ductile Fracture," *Metallurgical Transactions*, Vol. 6A, pp. 82, 1975.

16. McNelley, T.R., Lee, E.W. and Mills, M.E., "Superplasticity in a Thermomechanically Processed High-Mg, Al-Mg Alloy," *Metallurgical Transactions*, Vol. 17A, pp. 1035-1041.

17. Mathé, W., *Precipitate Coarsening During Overaging of 2519 Al-Cu Alloy: Application to Superplastic Response*, Master's Thesis, Naval Postgraduate School, Monterey, CA, March 1990.

18. Willig, V., and Heimendahl, M., "Problems of Particle Coarsening of Disk Shaped θ Particles in Aluminum Alloy 2219," Institut fur Wefkstoffwissenschaften 1 der Universitas Erlangen-Nurnberg, pp. 674-681.

19. *Metals Handbook*,American Society for Metals, 10th ed., Vol. 2, pp. 3-80, 1991.

20. Russell, K.C., and Aaronson, H.I, "Precipitation Processes in Solids," *The Metallurgical Society of AMIE*, pp. 87, 1978.

INITIAL DISTRIBUTION LIST

1.	Defense Technical Information Center Cameron Station Alexandria, VA 22304-6145	2
2.	Library, Code 52 Naval Postgraduate School Monterey, CA 93943-5002	2
3.	Naval Engineering, Code 34 Naval Postgraduate School Monterey, CA 93943-5100	1
4.	Department Chairman, Code ME/Kk Department of Mechanical Engineering Naval Postgraduate School Monterey, CA 93943-5000	1
5.	Professor T.R. McNelley, Code ME/Mc Department of Mechanical Engineering Naval Postgraduate School Monterey, CA 93943-5000	4
6.	Associate Professor R. Crooks, Code ME/Cc Department of Mechanical Engineering Naval Postgraduate School Monterey, CA 93943-5000	1
7.	LT. Jeffrey R. Dunlap 4787 Boykin Dr. N.Charleston, SC 02942	2